Low nitrate alleviates iron deficiency through regulating iron homeostasis in apple

Wei-Jian Sun[1], Xing-Long Ji[1], Zi-Quan Feng[1], Xun Wang[1], Jiu-Cheng Zhang[1], Wen-Jing Huang[2], Chun-Xiang You[1], Xiao-Fei Wang[3], and Yu-Jin Hao[1]

[1]Shandong Agricultural University
[2]Yunnan Academy of Agricultural Sciences
[3]Shandong Agricultural University, College of Horticulture Science and Engineering 61 Daizong Stree Tai-An, Shandong Province, CN 271018 86+538-8246692

April 28, 2020

Abstract

Iron (Fe) is an essential element for plant growth, development, and metabolism. Due to its lack of solubility and low bioavailability in soil, Fe levels are usually far below the optimum amount for most plants' growth and development. In apple production, excessive use of nitrogen fertilizer may cause iron chlorosis symptoms in the newly growing leaves, but the regulatory mechanism is unclear. In this study, it was found that low nitrate (NO3-, LN) application could alleviate the symptoms of Fe deficiency, LN treatment promoted lower the rhizosphere pH, which was beneficial for root Fe acquisition, meanwhile, LN treatment increased citrate and abscisic acid (ABA) accumulation in root, which promoted Fe transport from root to shoot and maintained Fe homeostasis. Moreover, RNA-Seq and qRT-PCR analysis showed that nitrate application caused differential expression of genes that were related to Fe uptake and transport as well as transcriptional regulators. In summary, our data reveal that low nitrate alleviated Fe deficiency through multiple pathway, which exhibits a new option for attenuating Fe deprivation by regulating the balance between nutrients.

Key words: iron deficiency, nitrate, citric acid, abscisic acid, apple

INTRODUCTION

Fe is an essential element for plant growth and development, due to its role in iron sulfur (FeS) proteins, ferredoxins, and various metabolic enzymes. It impacts various cellular processes, including photosynthesis, respiration, electron transfer reactions, and others (Connorton et al. 2017). Excessive Fe causes yellow-brown spots on the tips, edge, and interveinal of old leaves and represses plant growth, while Fe deficiency triggers chlorosis and reduces fruit yields (Álvarez-Fernández et al. 2003). Although soil contains abundant Fe, it is usually not available to plants due to its insoluble nature. This problem is exacerbated by alkaline and aerobic environmental conditions. Fe deficiency is a worldwide problem, with about 30% of the world's soil currently suffering from Fe deficiency, which severely restricts efforts to improve crop yield and quality (Marschner, 2011; Briat et al. 2015).

To cope with Fe deficiency, plants have evolved two major mechanisms to absorb Fe from the soil, known as strategy I for dicots and non-graminaceous monocots and strategy II for graminaceous monocots (Römheld & Marschner, 1986; Kobayashi & Nishizawa, 2012). Graminaceous plants, such as maize and rice, use strategy II, also known as the chelating strategy, to uptake Fe from the soil. These plants secrete phytosiderophores, which have high affinity for Fe, from their roots. Fe^{3+}-phytosiderophore chelates are imported by YS1 (Yellow Stripe 1) transporters in maize (Curie et al. 2001) and YSL15 transporters in rice (Inoue et al. 2009). In contrast, non-graminaceous plants, such as *Arabidopsis thaliana* and tomato, use strategy I, also known

as the reducing strategy, to absorb Fe from rhizosphere. In this strategy, plasma membrane H^+-ATPases first acidify the rhizosphere and facilitate Fe solubilization by pumping protons (H^+) into root rhizosphere. Next, FRO2 (Ferric Reduction Oxidase 2) at the plasma membrane reduces Fe^{3+} to Fe^{2+}, which is then transported across the membrane by IRT1 (Iron-Regulated Transporter 1) (Jeong & Guerinot, 2009; Santi & Schmidt, 2009; Ivanov et al. 2012; Kobayashi and Nishizawa, 2012; Jeong et al. 2017). Finally, Fe is transported to the shoot through long-distance transportation, which requires many genes, including *NAS* (Nicotianamine Synthesis) (Haydon & Cobbett, 2007; Jeong and Guerinot, 2009), *FRD3* (Ferric Redictase Defective3) (Durrett et al. 2007; Jeong and Guerinot, 2009), *YSL* (Yellow Stripe-Like) (Waters et al. 2006; Haydon & Cobbett, 2007), *OPT3* (Oligopeptide Transporter3) (Stacey et al. 2008; Ivanov et al. 2012), and *FPN1* (Ferroportin1) (Morrissey et al. 2009; Ivanov et al. 2012). Despite their obvious differences, evidence shows that the two strategies share several components. Strategy I plants have been found to secret chelators to rhizosphere, such as phenolics, flavonoids and flavins, as a typical feature of strategy II plants (Fourcroy et al. 2014; Connorton et al. 2017; Grillet & Schmidt, 2019). Additionally, a functional homologue of *IRT1* has been found in rice, which mediates Fe^{2+} uptake under low oxygen conditions (Ishimaru et al. 2006).

Over the past few decades, significant progress had been made in uncovering the mitigation and regulation mechanisms of iron deficiency in plants. For strategy I plants, rhizosphere acidification and Fe^{3+} reduction are essential processes which enable Fe transport from the soil to roots. Upon exposure to Fe deprivation conditions, protons are released from H^+-ATPase plasma membrane pumps to acidify the soil and increase the solubility of Fe. Some H^+-ATPases (AHA) genes are induced under Fe deficiency and are therefore thought to function in Fe-deficiency responses (Santi et al. 2008; 2009). After acidification, free ferric Fe is reduced to ferrous ions by FRO2 (Robinson et al. 1999). In*Arabidopsis* , the FRO family contains eight members, each of which are thought to play different functions (Mukherjee et al. 2006). Once reduced by FRO2, Fe^{2+} is transported into the root by IRT1, a member of the ZIP family (Guerinot. 2000). Knock-outs of*IRT1* result in Fe deficiency accompanied by cell differentiation defects, which points to the important role played by *IRT1* (Henriques et al. 2002). Both *FRO2* and I*RT1* are regulated by *FIT* , at the transcriptional level and the post-transcriptional level, respectively (Colangelo & Guerinot. 2004). Another process involved in strategy I is the excretion of Fe-mobilizing coumarins under high pH conditions. The biosynthesis and secretion of these coumarins involve *F6'H1* (Feruloyl-CoA 6'-Hydroxylase1), *S8H* (Scopoletin 8-hydroxylase), *CYP82C4* (Cytochrome P450, Family 82, Subfamily C, Polypeptide 4), *PDR9* (Pleiotropic Drug Resistance 9), and *BGLU42* (Beta Glucosidase 42) (Fourcroy et al., 2014; Zamioudis et al., 2014; Schmid et al., 2014, Rajniak et al., 2018; Siwinska et al., 2018; Tsai et al., 2018). Once Fe enters the plant, it must be safely transported to multiple parts of plant, which requires chelators, such as citrate and nicotianamine (NA) (Haydon & Cobbett. 2007; Curie et al. 2009).

Organic acids, especially citrate, are the main metal chelators in xylem and function in metal ion transportation (Brown et al, 1971; Rellan-Alvarez et al, 2010). Fe^{3+}-citrate has been proposed to be the main form of Fe present in xylem exudates (Grotz & Guerinot. 2006). *FRD3* is a MATE family member, which has been proposed to play a role in transporting citrate into xylem (Durrett et al. 2007; Morrissey et al. 2009). *Arabidopsis* mutants with abolished function of *FRD3* show various Fe deficiency symptoms, while overexpression of *FRD3* in rice enhances Fe mobility, resulting in elevated levels of Fe in the endosperm (Roschzttardtz et al. 2011; Wu et al. 2018). NA is a precursor of MA (Mugineic acid), which complexes with Fe and is required for unloading it from vascular tissues (Haydon & Cobbett. 2007; Clemens. 2019). *NAS* genes are responsible for NA synthesis. In *Arabidopsis* , *AtNAS1* is involved in the synthesis of NA from SAM (S-adenosyl-L-methionine) (Haydon & Cobbett. 2007). *NAS* genes are also upregulated in shoots and roots under Fe deficiency (Wintz et al. 2003). YSL transporters are hypothesized to transport the Fe-NA complex from the phloem to surrounding parenchyma, and YSL1 and YSL3 are suggested to be involved in the translocation of other metals (Waters et al. 2006; Curie et al. 2009; Chu et al. 2010; Kumar et al. 2017).

Fe-deficiency induces gene expression associated with ethylene synthesis and signaling processes in roots, which causes the upregulation of Fe-related genes, such as *AtFIT* , *AtFRO2* , *AtIRT1* ,*AtNAS1* , *AtFRD3* , and others (Lucena et al. 2006; Garcia et al. 2010). A similar mechanism has been found in rice, where

Fe-deficiency induces abscisic acid accumulation rapidly in roots (Wu et al. 2011). Exogenous 0.5 μM ABA promotes apoplastic Fe reutilization, while treatment with ABA upregulates expression of *AtFRD3* ,*AtYSL2* , and *AtNAS1* and increases Fe content in xylem sap, indicating that ABA promotes transport of Fe from root to shoot (Lei et al. 2014). Fe-deficiency also increases NO (Nitric Oxide) in roots, which is involved in upregulation of Fe-related genes (Chen et al. 2010; García et al. 2010). Zhu et al. (2017) found that NaCl mitigates iron deficiency by facilitating Fe reutilization and translocation from root cell wall to shoots.

Many transcription factors (TFs) participate in the regulation of Fe deficiency responses. Among them, bHLH (basic helix-loop-helix) transcription factors are the predominant family (Heim et al. 2003; Gao et al. 2019). In *Arabidopsis* , expression of *FIT/bHLH29*(Fe-Deficiency Induced Transcription Factor) is induced by Fe-deficiency in roots, which then regulates the expression of *AtIRT1* and*AtFRO2* , together with *AtbHLH38* and *AtbHLH39* (Li et al. 2016). In addition, FIT interacts with EIN3 (Ethylene Insensitive 3) to regulate Fe uptake (Lingam et al. 2011). The bHLH105/ILR3 (IAA-Leucine Resistant 3) is proposed to act as both transcriptional activator and repressor, and it may be a core TF for the transcriptional regulatory network that controls Fe homeostasis in *Arabidopsis*(Tissot et al. 2019). Additionally, ILR3 also interacts with bHLH104 to modulate Fe homeostasis in *Arabidopsis* (Zhang et al. 2015). Zhou et al. (2019) reported that MdbHLH104 is stabilized by the SUMO E3 ligase MdSIZ1 to regulate plasma membrane H^+-ATPase activity and Fe homeostasis. In apple, overexpression of the*MdbHLH104* gene enhances the tolerance to Fe deficiency (Zhao et al. 2016a). Two BTB scaffold proteins, MdBT1 and MdBT2, target MdbHLH104 and negatively regulate the stability of MdbHLH104 to affect plasma membrane H^+-ATPase activity and Fe homeostasis (Zhao et al. 2016b). In addition, other TFs, such as MYB and WRKY are required for plant growth under Fe-deficient conditions (Palmer et al. 2013; Yan et al. 2016; Wang et al. 2018).

Nitrogen is an indispensable nutrient for plants, with nitrate representing the main bioavailable form for land plants. Nitrate (NO_3^-) also acts as a vital signaling molecule that modulates various growth and development processes of plants, including seed germination, flowering, shoot branching, and root development (Bouguyon et al. 2016; Yan et al. 2016; Canales et al. 2017; Fredes et al. 2019). In potato (*Sohmum tuherosum* L.), interrupting the N supply increases ABA content, which slowly recovers to normal levels after N levels are restored (Krauss. 1978). In wheat seedlings, nitrogen deficiency results in the rapid accumulation of ABA, especially in roots (Teplova et al. 1998). There are also interactions between nitrate and other nutrient signaling pathways. Liu et al. (2017) found that Ca^{2+} signaling sensor CPKs interact with NLP7 (NIN-Like Protein 7) to modulate nitrate response. Recent research also found that nitrate acts as a signal to coordinate N-P nutrient balance in rice (*Oryza sativa* L.) (Hu et al. 2019).

Here, we investigated the effect of nitrate on Fe deficiency and found that the application of nitrate influenced Fe deficiency response. The regulatory mechanisms behind this relationship were also investigated, which sheds new light on the interaction between nitrate and iron in apple and other species.

MATERIALS AND METHODS

Plant material and growth conditions

'*Pinyiensis* ' (*Malus hupehensis* Rehd.) and*Arabidopsis thaliana* (Columbia ecotype) were used in this study. '*Pinyiensis* ' fruits were collected from National Engineering Research Center for Apple of Shandong Agricultural University and the seeds were harvest. '*Pinyiensis* ' seeds were first laminated for 30 days using wet sand in 4, dark. Then the seeds were planting onto the nursery (substrate: meteorite 3:1) for germination at 25. After germination the seedlings were cultivated on nursery for 2 weeks and then transferred into vermiculite moistened with the complete nutrient. The complete nutrient was composed of following components:10 μM MnSO4; 100 μM H_3BO_3; 0.1 μM CuSO4; 0.1 μM Na2MoO4; 30 μM ZnSO4; 5 μM KI; 0.1 μM CoCl2; 4 mM CaCl2; 1 mM MgSO4; 1 mM KH2PO4; 50 μM Fe(III)-EDTA; 5 mM KNO3. For phenotypic analysis, 6-week-old seedlings with the same growth status were transplanted to a new vermiculite pot and subjected with following treatments for 3 weeks: 0.5 mM KNO3 + 50 μM Fe, 15 mM KNO3 + 50 μM Fe, 0.5 mM KNO3-Fe (-Fe solution supplemented with 200 μM ferrozine) or 15 mM KNO3 -Fe (-Fe solution supplemented with 200 μM ferrozine), with KCl was added to maintain the same K^+concentration (15 mM).

Seedlings were cultivated in a controlled environment: 25, 60% relative humidity and a 16h day/8h night rhythm. The treatment solutions were renewed every 7 days.

Columbia ecotype *Arabidopsis thaliana* seeds were surface-sterilized and germinated on substrate containing agar and 1/2 MS (Murashige & Skoog, 1962) nutrient. After 1 week of growth, seedlings were transferred to vermiculite moistened with complete nutrient for 1 week. The vermiculite was washed with deionized water from top to bottom for 4 times before subjected with following treatments: 0.2 mM KNO_3 + 50 µM Fe, 20 mM KNO_3 + 50 µM Fe, 0.2 mM KNO_3 -Fe (-Fe solution supplemented with 200 µM ferrozine), 20 mM KNO_3 -Fe (-Fe solution supplemented with 200 µM ferrozine), with KCl was added to maintain the same K^+ concentration (20 mM). Seedlings of similar rosette diameters were picked for treatment. The seedlings were cultivated in a growth room at 22, 65% relative humidity and a 16h day/8h night rhythm. The treatment solutions were renewed every 3 days.

Phenotypic analysis of exogenous application of citrate, malate and ABA

For phenotype analysis, 6-week-old seedlings with the same growth status were transplanted to a new vermiculite pot and subjected with different treatments for 3 weeks. Citric acid (citrate) (Aladdin, Shanghai, China) and malic acid (malate) (Aladdin, Shanghai, China) were dissolved with ddH_2O into 0.5 M stock solution and stored at 4. For exogenous citrate and malate treatment, the nutrient solutions are as follows: 15 mM KNO_3 + 200 µM ferrozine, 15 mM KNO_3 + 200 µM ferrozine + 0.5 mM citrate/malate, 0.5 mM KNO_3 + 200 µM ferrozine, 0.5 mM KNO_3 + 200 µM ferrozine + 0.5 mM citrate/malate, with KCl was added to maintain the same K^+ concentration (15 mM). Abscisic acid (BBI, Toronto, Canada) was dissolved with 100 µL ethanol and diluted with ddH_2O into 5 mM stock solution, stored in brown reagent bottle at 4. ddH_2O containing 100 µL ethanol was used as control. For exogenous ABA treatment, the nutrient solutions are as follows: 15 mM KNO_3 + 200 µM ferrozine + control, 15 mM KNO_3 + 200 µM ferrozine + 1 µM ABA, 0.5 mM KNO_3 + 200 µM ferrozine + control, 0.5 mM KNO_3 + 200 µM ferrozine + 1 µM ABA, with KCl was added to maintain the same K^+ concentration (15 mM). Each treatment contained at least 3 biological replicates; each replicate contained 10 plant samples.

Field experiments of nitrate treatment on 'Fuji' trees

For field experiment, 2-year-old 'Fuji' trees were selected as experimental material. 'Fuji' trees were planted at National Engineering Research Center for Apple of Shandong Agricultural University. Line spacing × plant spacing is ˜ 2 meters × 0.7 meters. Each line contains 11 trees. Since April 2018, the trees were treated with 10, 30, 60 or 120g KNO_3 fertilizer per plant, respectively, with KCl was added to maintain the same K^+ concentration. KNO_3 fertilizer was applied to the left side of the tree, near the root. The treatment was performed once a month until June. KNO_3 fertilizer was purchased from Shandong Agricultural University Fertilizer Technology Co., Ltd. (Tai' an, China).

Chlorophyll content measurement

For '*Pinyiensis* ' seedlings, chlorophyll content was estimated by a portable chlorophyll meter (CL01,*Hansatech* , Kings Lynn, UK). The result was expressed as "chlorophyll index" (Cassol et al. 2008). For *Arabidopsis* seedlings shoots and 'Fuji' tree leaves, chlorophyll content was extracted and measured as previously described (Porra et al.1989).

Metal content analysis

For total Fe content analysis, plant samples were collected and washed with 2 mM $CaCl_2$. The samples were firstly dried at 105 for 0.5 h and subsequently oven-dried at 70. The oven-dried samples were ground into powder and its dry weight was recorded. Next, the powder was put into 50 mL conical flask dispersed in 5 mL concentrated H_2SO_4, incubated at room temperature (˜24) for 12 h. Finally, the samples were heated to 330 and digested by slowly adding 10 mL 30% H_2O_2 until it was clear (Smolders et al. 1997). The digested liquid was filtered with 0.45 µM filter and filtrate was diluted with ddH_2O. Total Fe content was assessment by inductively coupled plasma optical emission spectrometer (ICP-OES, iCAP 7400, Thermo Fisher Scientific, Bremen, Germany).

4

Water-soluble Fe was extracted according to Cassin *et al* . (2009). Briefly, samples were weighed and ground in liquid nitrogen. Then, 10 mL deionized water was added at room temperature. Subsequently, it was centrifugation for 10 min and the supernatant was collected. The Fe concentration of the supernatant was measured using the same method as total Fe.

Root FCR activity measurement

The root FCR (Ferric-chelate reductase) activity was quantified using a ferrozine assay (Schikora & Schmidt, 2001). The roots were initially washed in 0.5 mM $CaSO_4$ for 5 min. Then the whole roots were excised, weighed and put into a 50 mL tube with 50 mL assay solution (pH 5.8). The assay solution contained 0.5 mM ferrozine (FRZ), 0.5 mM CaSO4, 0.5 mM Fe-EDTA (ethylenediaminetetraacetic acid). The tubes were put at room temperature (~24) in dark for 1 h, with a handy shake every 10 min. The absorbance of the solutions was determined by a spectrophotometer (UV 1800, Shimadzu, Japan) at 562 nm. The reduction rate was calculated after subtraction of the appropriate blanks (assay solution without roots). The rate of root FCR activity was calculated as moles of Fe_2C-ferrozine per gram of fresh weight per hour. Each treatment contained at least 3 biological replicates.

Rhizosphere pH measurement

For rhizosphere pH measurement, seedlings were hydroponics with 0.5 mM KNO_3 + 50 µM Fe, 15 mM KNO_3 + 50 µM Fe, 0.5 mM KNO_3-Fe (-Fe solution supplemented with 200 µM ferrozine), 15 mM KNO_3-Fe (-Fe solution supplemented with 200 µM ferrozine) treatments. The pH was measured daily with a pH electrode (PHS-3C, INESA Scientific Instrument Co., Ltd, Shanghai, China). Each treatment contained 10 biological replicates.

Determination of organic acid content

MCW (Methanol-Chloroform-Water)-method was used to extract tissue metabolites, according to Ma et al. (2017). Weigh 50~100 mg (Fresh weight, Fw) tissue powder (kept in liquid nitrogen) to a precooled plastic 2 mL centrifuge tube. Add 0.7 mL 7:3 Methanol-Chloroform (-20) to the sample plus 20 µL PIPES (300 µmol/L) as the internal standard (IS). Then, add two metal beads to homogenize the samples on the grinding mill at a frequency of 40 repetitions/s for 5 min. The mixture is incubated at -20 for 2 h with a shaking every other 30 min. Subsequently, add 0.56 mL ice-cold ddH_2O to the mixture, vigorously vortex the tube and centrifuge for 10 min at 8000 rpm at 4. Transfer the upper, aqueous methanol-H_2O phase to a new precooled 2 mL centrifuge tube and add 0.56 mL ice-cold ddH_2O to the residue and repeat the extraction step; then combine the second upper phase with the first one. The viscous, high-molecular mass components are filtered by 0.45 µM cellulose acetate centrifuge filters. Dry the extracts with N_2 at room temperature (~24) and re-dissolve the dry extract with 200 µL ddH_2O, as the concentrated samples. Finally, dilute the concentrated samples 20 times with ddH_2O (10 µL concentrated sample +190 µL ddH_2O) and the samples for quantifying is ready. LC-MS/MS (TSQ Quantum Access MAX, Thermo Scientific, America) was used to inspect organic acids content (Ma et al. 2014, 2017).

Endogenous ABA assay

ABA content was determined by HPLC-electrospray ionization-tandem mass spectrometry method (Chen et al. 2011). Internal ABA was extracted according to the method and made some modulation. Plant samples were harvest, processed by vacuum freeze drying by a lyophilizer (FDU-1110, EYELA, Tokyo, Japan) and ground in liquid nitrogen, then the samples were weighed and transferred to a 50 mL centrifuge tube. Added 15 mL methanol containing 20% ddH_2O (v/v) at 4 for 12 h for extraction. $[^2H_6]$ ABA (50 ng/g) was added to plant samples as internal standard (IS) prior to grinding. After centrifugation at 10,000 rpm at 4 for 20 min, the supernatant was collected and passed through a C-18 (100 mg) SPE cartridge, which was preconditioned with 8 mL ddH_2O, 8 mL methanol, and 8 mL methanol containing 20% ddH_2O (v/v). The elution was pooled, dried with nitrogen gas and re-dissolved with 2 mL ddH_2O. The solution was acidified with 240 µL, 0.1 mol/L HCL and extracted with ethyl ether (4 × 1 mL). The organic phases were combined, dried by nitrogen gas and re-dissolved with 80 µL acetonitrile (ACN). To the resulting solution, 10 µL trimethylamine

(TEA, 20 μmol·mL^{-1}) and 10 μL 3-bromoactonyltrimethylammonium bromide (BTA, 20 μmol·mL^{-1}) were added. The reaction solution was vortexed for 30 min to mix up and dried with nitrogen gas and re-dissolved with 200 μL ACN containing 20% (v/v) ddH$_2$O. 20 μL of the solution was subjected to HPLC-electrospray ionization-tandem mass spectrometry analysis. Each treatment contained at least 3 biological repeats and each repeat contained 3 shoots or roots samples. Each testing sample contained 3 replicates.

Nitrate content and total nitrogen content determination

Nitrate content was determined by the hydrazine reduction method according to Cao et al. (2017). In brief, the samples were collected, washed and ground into powder using mortar. The powder was transferred to 2 mL centrifuge tube and 1 mL ddH$_2$O was added, following by boiling at 100 for 30 min. The cooled sample was centrifuged at 12000 rpm for 10 min and 400 μL was collected for analysis. The nitrate content was detected using AutoAnalyzer 3 continuous flow analytical system (AA3, SEAL Analytical, Germany). Total nitrogen content was detected by Kjeldahl method based on a previously published description (Magomya et al. 2014).

RNA-seq analyses of '*Pinyiensis*' and bioinformatics analysis

Two sets of samples, comprising one treatment (15 mM KNO$_3$) and one control (15 mM KCl), with three biological replicates each were subjected to RNA-seq. Each biological replicate contained 10 seedling samples. Seedlings with the same growth status were pre-treated with 15 mM KCl for 3 days and subsequently, one set of seedlings were treated with 15 mM KNO$_3$ and the other set of seedlings were continue processed with 15 mM KCl (both under low Fe treatment). After 12 h treatment, root samples were collected and frozen in liquid nitrogen, respectively. Samples were ground into powder in mortar and stored at -80. Total RNA was extracted using mirVana miRNA ISOlation Kit Ambion-1561 (ABI, Carlsbad, USA) following the manufacturer's protocol. RNA integrity was evaluated using the Agilent 2100 Bioanalyzer (Agilent Technologies, Santa Clara, CA, USA). The samples with RNA Integrity Number (RIN) [?] 7 were subjected to the subsequent analysis. The libraries were constructed using TruSeq Stranded mRNA LTSample Prep Kit (Illumina, San Diego, CA, USA) according to the manufacturer' s instructions. Total RNAs eliminating mRNA were used for strand-specific library construction. Then these libraries were sequenced on the Illumina sequencing platform (HiSeq^{TM}2500) by OE Biotechnology (Shanghai, China). Reads obtained from sequencing were filtered to remove adaptors and low-quality reads using Trimmomatic (Bolger et al. 2014). The clean reads from each sample were mapped to the reference genome with hisat2.

Gene expression analysis by qRT-PCR

For gene expression analysis, seedlings of same growth status were treated with 0.5 mM KNO$_3$ + 50 μM Fe, 15 mM KNO$_3$ + 50 μM Fe, 0.5 mM KNO$_3$ -Fe (-Fe solution supplemented with 200 μM ferrozine) or 15 mM KNO$_3$ -Fe (-Fe solution supplemented with 200 μM ferrozine) solutions for 1, 3, 5 and 7 days, respectively. Roots were collected, washed and frozen in liquid nitrogen. The roots were grinded into powder with a mortar and pestle. Total RNA was extracted with an Omini Plant RNA Kit (CWBIO, Beijing, China) following the manufacturer's protocol. cDNA was prepared from 1 μg total RNA using the PrimeScript^{TM} RT reagent Kit (Takara, Dalian, China). An Ultra SYBR Mixture (CWBIO, Beijing, China) was used to detect the expression levels of genes using qRT-PCR (ABI, StepOnePlus, USA). *MdActin* (GenBank accession No.:CN938023) was selected as an internal control gene. Results were based on the average of three replicate experiments. All primers used in this study was shown in Table 1.

Statistical analysis

Data were analyzed by one-way analysis of variance (ANOVA) and the data were compared by Duncan's multiple range test. Different letters indicate the data were statistically different at *P < 0.05* level.

RESULTS

Nitrate inhibits iron accumulation in the newly growing leaves of apple

6

Two-year-old trees of the apple cultivar 'Fuji' were treated with 10, 30, 60, or 120 g nitrate fertilizer per plant. We found that increased nitrate application resulted in more severe iron deficiency symptoms in new leaves (Fig. S1), while chlorophyll content gradually decreased (Fig. S2). To further explore the effects of nitrate on iron uptake in apple, apple seedlings were treated with +Fe and -Fe nutrient solutions containing high concentration of nitrate (HN, 15 mM) and low concentration of nitrate (LN, 0.5 mM). To create an ideal experimental environment, we chose vermiculite rather than soil to cultivate the seedlings, which has no soluble Fe but contains Fe_2O_3. The application of ferrozine (FRZ) in -Fe treatments enabled chelation of Fe^{2+} which limits the uptake of Fe^{2+}. After 15 days, the newly growing leaves showed severe chlorosis and reduced chlorophyll content under HN-Fe treatment (Fig. 1a, b, c). By contrast, slight chlorosis was observed under LN-Fe treatment. Additionally, when there was no iron shortage, LN treatment seedlings had a lower chlorophyll content than HN treatment seedlings (Fig. 1a, c). These results suggested that LN treatment alleviates iron deficiency in seedlings. Meanwhile, the soluble Fe content of both newly growing leaves (Fig. 1d) and roots (Fig. 1e) significantly increased under LN-Fe treatment, even though vermiculite has very little soluble Fe. Additionally, soluble Fe content in young leaves of seedlings which were treated with LN solution with sufficient iron supplementation was higher than seedlings which were treated with HN solution with sufficient iron supplement treatment (Fig. 1d). These results implied that LN-triggered alleviation of Fe deficiency may be due to an increase in iron reutilization.

Nitrate supply level influences rhizosphere pH value and Fe solubility

Seedlings treated with HN showed an increase of rhizosphere pH under both iron sufficient and deficient conditions, while the rhizosphere pH of the LN treatment was significantly lower than HN treatment (Fig. 2d, e). HN treatment led to higher amount of alkaline in the rhizosphere, which caused reduced solubility of iron in the rhizosphere and more difficulty for seedlings to absorb iron. There was no significant difference of pH when there were no plants in the solutions (Fig. 2c). As shown in Fig. 2, seedling under HN treatment had a higher FCR (Ferric-chelate Reductase) activity under both +Fe and -Fe conditions, while seedling under LN treatment had a lower FCR activity under both +Fe and -Fe conditions (Fig. 2a, b). The above results demonstrated that HN treatment exacerbates iron deficiency symptoms, while LN treatment attenuates plant Fe deficiency symptoms, partially by affecting rhizosphere pH.

Low nitrate treatment promotes iron transportation from root to shoot

Under Fe adequate conditions, we found that there was no significant difference in total Fe content in new leaves and roots under either HN or LN treatment. By contrast, under Fe deficient conditions, LN treatment remarkably increased total Fe content both in newly growing leaves and roots (Fig. 3a, b). In addition, the Fe content was higher in stems of plants under LN-Fe treatment than that under HN-Fe treatment (Fig. 3c). Nitrogen content analysis suggested that seedlings under HN-Fe treatment had a higher nitrate and total nitrogen content than that of LN-Fe treatment (Fig. S3a, b, c). Furthermore, gene expression analysis found that the expression of *MdFRD3* and *MdMATE43* , which are associated with vascular Fe loading and unloading, were dramatically increased by LN treatment (Fig. 3d, e). Early on in Fe deficiency (1 day), LN treatment promoted the expression of *MdNAS1* (Fig. 3f), suggesting that LN-promoted iron transportation might result from LN-induced upregulation of genes related with Fe-chelator formation and transportation.

Citrate participates in nitrate-alleviated iron deficiency

Since citrate is known to function in the transport of Fe from root to shoot (Grotz & Guerinot. 2006), it seems likely that it may participate in the nitrate-regulated iron deficiency response in apple. To assess this possibility, we measured the contents of organic acids, including citrate (CIT) and malate (Mal), in apple roots. When Fe was adequate, HN treatment promoted citrate accumulation (Fig. 4a) but had no effects on malate content (Fig. 4b) in roots. Under Fe deficiency conditions, LN-treated roots showed a higher citrate content compared to HN-treated roots (Fig.4a), while no significant difference was observed in malate content (Fig. 4b). Citrate and malate content showed no significant difference in leaves under HN-Fe and LN-Fe treatment (Fig. S4a, b). These results indicated that low nitrate affects citrate content but not malate accumulation in roots.

7

To further verify whether citrate participated in LN-alleviated Fe deficiency, exogenous citrate was applied to Fe deficient plants. As shown in Fig. 4, exogenous citrate noticeably alleviated HN-mediated Fe deficiency, resulting in an increase in chlorophyll content (Fig. 4c, d), increased total Fe content in newly growing leaves (Fig. 4e), and decreased total Fe content in roots (Fig. 4f). The above results suggested that exogenous citrate was able to alleviate Fe deficiency by facilitating Fe transportation from root to shoot.

Transcriptome profiling of genes related to iron utilization in response to nitrate treatment

To better understand and explain the mechanism surrounding nitrate's effects on iron deficiency responses, an RNA-seq analysis was carried out using seedlings of crabapple '*Pinyiensis*' treated with different nitrate concentrations. All seedlings were pre-treated with KCl (15 mM) for 3 days. Then, half of the seedlings were exposed to HN (15 mM KNO_3, 5 μM Fe) treatment for 12 h, while another half were still treated with KCl (15mM, 5 μM Fe). RNA-seq analysis demonstrated that the expression levels of over 1600 genes changed in root samples (Fig. 5a). Among them, many genes were related to Fe uptake and transportation as well as Fe-related transcription regulators (Fig. 5b). The qRT-PCR analysis found that the plasma membrane H^+-ATPase gene *MdAHA2* was significantly induced by LN treatment, especially during the first day of iron deficiency (Fig. 6g). Moreover, the master transcriptional regulator of iron deficiency, *MdFIT*, was also induced by LN treatment (Fig. 6a). In the early stages of iron deficiency (1 day), the expression levels of*MdYSL1*, *MdYSL3*, *MdFER1* and *MdNAS1* were higher in LN treatment than in HN treatment (Fig. 6d, c, b; Fig. 3f). A vacuole Fe transporter gene, *MdNRAMP1* which transports Fe from the vacuole to the cytosol, was also significantly induced by LN treatment (Fig. 6f). These results indicated that the effect of LN on iron deficiency involved transcriptional regulation of multiple genes, including *MdAHA2*, which is involved in rhizosphere acidification, Fe transporter genes (*MdMATE43*, *MdNAS1*, *MdYSL1*) and*MdFIT* promote the expression of downstream genes related to iron deficiency. Further analysis also showed that the expression of some other metal ion related genes were affected by nitrate, including genes associated with Zn, Al, and Cu (Fig. S5a).

ABA alleviates nitrate-mediated Fe deficiency response

Previous studies have shown that nitrogen deficiency resulted in the accumulation of ABA (Krauss et al, 1978; Teplova et al, 1998) and our RNA-seq analysis also demonstrated that nitrate treatment affected the expression of genes related to ABA metabolism and signaling (Fig. S6). Considering ABA plays a role in alleviating Fe deficiency response (Lei et al. 2014), it seems likely that it is also involved in nitrate-regulated iron deficiency responses. To assess this possibility, endogenous ABA content was measured in seedlings of '*Pinyiensis*' under different nitrate treatments. ABA content increased with LN treatment in roots (Fig. 7b), while there was no apparent difference in ABA content in leaves (Fig. 7a). Meanwhile, exogenous ABA application partially rescued the chlorosis phenotype in response to HN treatment (Fig. 7c, d). These results indicated that LN promoted ABA accumulation in roots quickly, and that LN alleviated iron deficiency partially through promoting ABA accumulation in roots.

The regulatory mechanism of nitrate-mediated iron deficiency response is conserved in *Arabidopsis thaliana*

In order to determine whether nitrate-regulated iron deficiency response is conserved in different species, we conducted a similar iron deficiency experiment in *Arabidopsis*. After 7 days of treatment, the new *Arabidopsis* leaves were severely chlorotic under the HN-Fe treatment (Fig. 8a, b), while only slight chlorosis was observed under LN-Fe treatment, with a higher chlorophyll content than HN-Fe treatment (Fig. 8a, b, c). Additionally, we detected the total Fe content of shoots and found that the total Fe content was higher under LN treatment than that under HN treatment (Fig. 8d), which was consistent with the findings in '*Pinyiensis*'. The above results suggested that nitrate-mediated iron deficiency response is conserved in*Arabidopsis*, and it may be also conserved in other plant species.

DISCUSSION

Fe is an essential element for plants and is vital for plant growth and development. Plants have evolved com-

plicated mechanisms for regulating Fe homeostasis that involve multiple different pathways. In recent years, with the rapid development of biochemical and molecular biology technology, research on Fe absorption, transport, and utilization has yielded many new insights (Jeong & Guerinot, 2009; Kobayashi & Nishizawa, 2012; Connorton et al. 2017). Many of the upstream regulatory mechanisms have been elucidated in recent years, including the role of bHLH and MYB transcriptional factors (Palmer et al. 2013; Gao et al. 2019). Moreover, it has been shown that plant hormones, such as ABA and ethylene, as well as environmental factors, such as NO and phosphate, participate in the regulation of Fe homeostasis (Hirsch et al. 2006; Chen et al. 2010; García et al. 2010; Lei et al. 2014; Romera et al. 2017).

As a common element found in soil, nitrogen plays an important role in plant yield. Excessive use of nitrogen fertilizer may cause an imbalance of nutrients (ZhongYang. 2016). However, the exact mechanisms behind the symptoms caused by these imbalances have not been fully explored. In this study, we analyzed the effect of nitrate on the regulation of Fe homeostasis. We found that nitrate could affect Fe uptake both directly and indirectly by affecting citrate levels and ABA accumulation (Fig. 4, Fig. 7). These findings may lead to new strategies to attenuate Fe deficiency by controlling the input of other nutrients in the future.

Previous studies have indicated that plants evolved two different strategies to uptake Fe from soil, although both of these strategies share some overlap (Römheld & Marschner. 1986; Connorton et al, 2017; Grillet & Schmidt. 2019). Our results further verified that apple mainly uses strategy I to uptake Fe from soil, which mainly involved differential expression of *MdAHA2* and *MdFRO2* (Fig. 6g, h). Moreover, the transcriptome and qRT-PCR data showed that the expression of *MdCYP82C4* , which is involved in the biosynthesis of Fe-mobilizing coumarins, is repressed by HN treatment (Fig. 5b, Fig. 6e), indicating that apple also employs chelator-based Fe acquisition strategies (Schmid et al. 2014; Rajniak et al. 2018). Our results also demonstrated that low-nitrate treatment facilitates Fe activation by regulating rhizosphere pH (Fig. 2), while the expression of *MdFRO2* was higher under high-nitrate treatment (Fig. 6h). We assume that high-nitrate treatment leads to a higher pH of rhizosphere and represses Fe uptake, which pushes a higher expression level of root *MdFRO2* to improve the efficiency of iron absorption. Low-nitrate treatment may also alleviate Fe deficiency by regulating citric acid and ABA accumulation in roots (Fig. 4, Fig. 7), which affects Fe reutilization and long-distance transport.

Plant Fe homeostasis regulation is a complicated process and there are likely other regulatory pathways involved which were not identified in this study. NO plays a positive role in regulating Fe deficiency, and evidence has shown that nitrate is the precursor of NO, which increases in roots upon nitrate addition (Bethke et al. 2004; García et al. 2010). Ethylene was shown to play a role in the regulation of Fe deficiency (Lucena et al. 2006; Wu et al. 2011), when Scheible et al. (2004) found that many genes involved in ethylene synthesis and perception were downregulated by nitrate addition. Nitrate addition also induces the biosynthesis of CKs by regulating expression of *IPT3* . The induced CKs are then able to repress the expression of *IRT1* , *FRO2* , and *FIT* and negatively regulate iron uptake in roots (Miyawaki et al. 2004; Takei et al. 2004; Séguéla et al. 2008). Taken together, these findings indicate that the effects of nitrate on Fe homeostasis are multifaceted and highly coordinated. We utilized RNA-seq analysis and found that the nitrate signal may be connected with multiple phytohormones, including ABA, ethylene, and CKs (Fig. S5b). LN treatment significantly increased Fe content in the leaves, and significantly increased the Fe content in stem under -Fe conditions (Fig. 3a, c), indicating that this treatment can promote Fe transport from root to shoot through xylem. Many genes are likely involved in this process, including *MdNRAMP1* , *MdNAS1* , *MdYSL1* , and *MdMATE43* . *NRAMP1* plays an important role in exporting Fe stored in vacuole, while *NAS1* and *YSL1* transport Fe (Wintz et al. 2003; Haydon & Cobbett. 2007; Kumar et al. 2017; Bastow et al. 2018; Clemens. 2019). *MATE43* is a homolog of *AtFRD3* which is responsible for transporting citrate into xylem (Durrett et al. 2007; Morrissey et al. 2009; Wang et al. 2018). It is well known that the chelation of Fe by metal binding compounds is the primary mechanism for long-distance transport. Upon reaching the vasculature, Fe is subsequently loaded into the xylem where it is chelated with citrate and transported to aerial plant tissues (Durrett et al. 2007; Clemens S. 2019). In this study, it was found that citrate promoted Fe transport from root to shoot, lending further support to earlier findings which showed citrate acts as an iron chelator that mobilizes iron from roots to aerial tissues. Therefore, it seems likely that LN treatment

9

promotes the long-distance remobilization of Fe from root vacuoles, thereby attenuating the chlorosis caused by Fe deprivation.

It has been well-documented that there is mutual regulation between different plant nutrients. Gratz et al. (2019) demonstrated that Fe deficiency induced cytosolic Ca^{2+} concentration and Ca^{2+} triggered CBL1/9-mediated activation of CIPK11. This in turn led to the phosphorylation and activation of FIT proteins, enabling the Fe deficiency response. In tomato, Pi transporter gene *Lept2* was up regulated by nitrate treatment, suggesting a potential coordination of nitrate and Pi uptake in plant, while Pi was indicated to antagonist Fe (Wang et al. 2001; Hirsch et al. 2006; Zheng et al. 2009). In this study, we found that citrate played a dominant role in the process of nitrate-regulated Fe deficiency response in apple, while malate had no significant effect. However, malate was shown to affect Fe acquisition in *Arabidopsis* (Mora-Macías et al. 2017), suggesting that Fe absorption and transport are not completely conserved between different species.

Based on our Fe deficiency response data, we constructed a model to integrate the roles played by different transcription factors and transporters (Fig. 9). Under Fe deficiency conditions, LN enhanced the expression of *MdAHA2* which aided rhizosphere acidification and increased the solubility of Fe, enabling more efficient uptake. Meanwhile, LN increased plant ABA content, which facilitated cell wall Fe reutilization and transport from root to shoot. Moreover, LN promoted citric acid accumulation in root and promoted Fe transport to shoot through xylem in the form of Fe^{3+}-citrate. LN treatment also promoted the expression of *MdFRD3* and *MdMAE43* , which facilitated citrate-based transport of Fe into xylem. Additionally, LN enhanced the expression of *MdNAS1* , which is responsible for NA synthesis and promoted Fe transport to shoot through phloem in the form of Fe^{2+}-NA. LN also upregulated the expression of the transcription factor *MdFIT* , which plays an important role in the Fe homeostasis regulatory network. Further study is required to understand the exact mechanisms underlying the effect of nitrate on these different genes. Overall, this study describes a possible model by which nitrate levels affect the uptake and transportation of Fe. These finding provide new knowledge about how nitrogen, hormones, and organic acids coordinate iron balance under iron deficient conditions.

REFFERENCES

Álvarez-Fernández, A., Paniagua, P., Abadía, J., & Abadía, A. (2003). Effects of Fe deficiency chlorosis on yield and fruit quality in peach (Prunus persica L. Batsch). *Journal of Agricultural and Food Chemistry* **51** , 5738-5744.

Bastow, E. L., De La Torre, V. S. G., Maclean, A. E., Green, R. T., Merlot, S., Thomine, S., & Balk, J. (2018). Vacuolar iron stores gated by NRAMP3 and NRAMP4 are the primary source of iron in germinating seeds. *Plant Physiology* **177** , 1267-1276.

Bethke, P. C., Badger, M. R., & Jones, R. L. (2004). Apoplastic synthesis of nitric oxide by plant tissues. *The Plant Cell* **16** , 332-341.

Bolger, A. M., Lohse, M., & Usadel, B. (2014). Trimmomatic: a flexible trimmer for Illumina sequence data. *Bioinformatics* **30,** 2114-2120.

Bouguyon, E., Perrine-Walker, F., Pervent1, M., Rochette1, J., Cuesta, C., Benkova, E., Martinière, A., Bach, L., Krouk, J., Gojon, A., & Nacry, P. (2016). Nitrate controls root development through posttranscriptional regulation of the NRT1. 1/NPF6. 3 transporter/sensor. *Plant physiology* **172,** 1237-1248.

Briat, J. F., Dubos, C., & Gaymard, F. (2015). Iron nutrition, biomass production, and plant product quality. *Trends in Plant Science* **20,** 33-40.

Brown, J. C., & Chaney, R. L. (1971). Effect of iron on the transport of citrate into the xylem of soybeans and tomatoes. *Plant Physiology* **47,** 836-840.

Canales, J., Contreras-López, O., Álvarez, J. M., & Gutiérrez, R. A. (2017). Nitrate induction of root hair density is mediated by TGA 1/TGA 4 and CPC transcription factors in Arabidopsis thaliana. *The Plant Journal* **92,** 305-316.

Cao, H., Qi, S., Sun, M., Li, Z., Yang, Y., Crawford, N. M., & Wang, Y. (2017). Overexpression of the maize ZmNLP6 and ZmNLP8 can complement the Arabidopsis nitrate regulatory mutant nlp7 by restoring nitrate signaling and assimilation. *Frontiers in Plant Science***8,** 1703.

Cassol, D., De Silva, F. S. P., Falqueto, A. R., & Bacarin, M. A. (2008). An evaluation of non-destructive methods to estimate total chlorophyll content. *Photosynthetica* **46** , 634.

Cassin, G., Mari, S., Curie, C., Briat, J.F. & Czernic, P. (2009) Increased sensitivity to iron deficiency in Arabidopsis thaliana over accumulating nicotianamine. *Journal of Experimental Botany***60,** 1249–1259.

Cataldo, D. A., McFadden, K. M., Garland, T. R., & Wildung, R. E. (1988). Organic constituents and complexation of nickel (II), iron (III), cadmium (II), and plutonium (IV) in soybean xylem exudates.*Plant Physiology* **86,** 734-739.

Chen, M. L., Huang, Y. Q., Liu, J. Q., Yuan, B. F., & Feng, Y. Q. (2011). Highly sensitive profiling assay of acidic plant hormones using a novel mass probe by capillary electrophoresis-time of flight-mass spectrometry. *Journal of Chromatography B* **879,** 938-944.

Chen, W. W., Yang, J. L., Qin, C., Jin, C. W., Mo, J. H., Ye, T., & Zheng, S. J. (2010). Nitric oxide acts downstream of auxin to trigger root ferric-chelate reductase activity in response to iron deficiency in Arabidopsis. *Plant Physiology* **154,** 810-819.

Clemens, S. (2019). Metal ligands in micronutrient acquisition and homeostasis. *Plant, cell & environment* **42** , 2902-2912.

Connorton, J. M., Balk, J., & Rodríguez-Celma, J. (2017). Iron homeostasis in plants–a brief overview. *Metallomics* **9,**813-823.

Colangelo, E. P., & Guerinot, M. L. (2004). The essential basic helix-loop-helix protein FIT1 is required for the iron deficiency response. *The Plant Cell* **16** , 3400-3412.

Curie, C., Panaviene, Z., Loulergue, C., Dellaporta, S. L., Briat, J. F., & Walker, E. L. (2001). Maize yellow stripe1 encodes a membrane protein directly involved in Fe (III) uptake. *Nature***409,** 346.

Curie, C., Cassin, G., Couch, D., Divol, F., Higuchi, K., Le Jean, M., Mission, J., Schikora, A., Czernic, P., & Mari, S. (2009). Metal movement within the plant: contribution of nicotianamine and yellow stripe 1-like transporters. *Annals of botany* **103** , 1-11.

Chu, H. H., Chiecko, J., Punshon, T., Lanzirotti, A., Lahner, B., Salt, D. E., & Walker, E. L. (2010). Successful reproduction requires the function of Arabidopsis Yellow Stripe-Like1 and Yellow Stripe-Like3 metal-nicotianamine transporters in both vegetative and reproductive structures. Plant physiology, 154(1), 197-210.

Durrett T.P., Gassmann W. & Rogers E.E. (2007) The FRD3-mediated efflux of citrate into the root vasculature is necessary for efficient iron translocation. *Plant Physiology* **144,** 197–205.

Fourcroy, P., Siso-Terraza, P., Sudre, D., Saviron, M., Reyt, G., Gaymard, F., Abadia, A., Abadia, J., Alvarez-Fernandez, A., & Briat, J. F. (2014). Involvement of the ABCG 37 transporter in secretion of scopoletin and derivatives by Arabidopsis roots in response to iron deficiency. *New Phytologist* **201,** 155-167.

Fredes, I., Moreno, S., Díaz, F. P., & Gutiérrez, R. A. (2019). Nitrate signaling and the control of Arabidopsis growth and development.*Current opinion in plant biology* **47,** 112-118.

Gao, F., Robe, K., Gaymard, F., Izquierdo, E., & Dubos, C. (2019). The transcriptional control of iron homeostasis in plants: a tale of bHLH transcription factors. *Frontiers in plant science* **10,** 6.

García, M. J., Lucena, C., Romera, F. J., Alcántara, E., & Pérez-Vicente, R. (2010). Ethylene and nitric oxide involvement in the up-regulation of key genes related to iron acquisition and homeostasis in Arabidopsis. *Journal of Experimental Botany* **61,**3885-3899.

Grotz, N., & Guerinot, M. L. (2006). Molecular aspects of Cu, Fe and Zn homeostasis in plants. *Biochimica et Biophysica Acta (BBA)-Molecular Cell Research* , **1763** , 595-608.

Gratz, R., Manishankar, P., Ivanov, R., Köster, P., Mohr, I., Trofimov, K., Steinhorst, L., Meiser , J., Mai, H. J., Drerup, M., Arendt, S., Holtkamp, M., Karst, U., Kudla, J., Bauer, P., & Brumbarova, T. (2019). CIPK11-dependent phosphorylation modulates FIT activity to promote Arabidopsis iron acquisition in response to calcium signaling.*Developmental cell* **48** , 726-740.

Grillet, L., & Schmidt, W. (2019). Iron acquisition strategies in land plants: not so different after all. *New Phytologist* .

Guerinot, M. L. (2000). The ZIP family of metal transporters.*Biochimica et Biophysica Acta (BBA)-Biomembranes* **1465** , 190-198.

Haydon M.J. & Cobbett C.S. (2007) Transporters of ligands for essential metal ions in plants. *New Phytologist* **174,** 499–506.

Heim, M. A., Jakoby, M., Werber, M., Martin, C., Weisshaar, B., & Bailey, P. C. (2003). The basic helix–loop–helix transcription factor family in plants: a genome-wide study of protein structure and functional diversity. *Molecular Biology and Evolution* **20,** 735-747.

Henriques, R., Jásik, J., Klein, M., Martinoia, E., Feller, U., Schell, J., Pasi, M. S. & Koncz, C. (2002). Knock-out of Arabidopsis metal transporter gene IRT1 results in iron deficiency accompanied by cell differentiation defects. Plant molecular biology 50, 587-597.

Hirsch, J., Marin, E., Floriani, M., Chiarenza, S., Richaud, P., Nussaume, L., & Thibaud, M. C. (2006). Phosphate deficiency promotes modification of iron distribution in Arabidopsis plants. Biochimie 88, 1767-1771.

Hu B., Jiang Z., Wang W., Qiu Y., Zhang Z., Liu Y., Li A., Gao X., Liu L., Qian Y., Huang X., Yu F., Kang S., Wang Y., Xie J., Cao S., Zhang L., Wang Y., Xie Q., Kopriva S. & Chu C. (2019). Nitrate–NRT1.1B–SPX4 cascade integrates nitrogen and phosphorus signalling networks in plants. *Nature Plants* . **5,** 401-413.

Inoue, H., Kobayashi, T., Nozoye, T., Takahashi, M., Kakei, Y., Suzuki, K., . . . & Nishizawa, N. K. (2009). Rice OsYSL15 is an iron-regulated iron (III)-deoxymugineic acid transporter expressed in the roots and is essential for iron uptake in early growth of the seedlings.*Journal of Biological Chemistry* **284,** 3470-3479.

Ishimaru, Y., Suzuki, M., Tsukamoto, T., Suzuki, K., Nakazono, M., Kobayashi, T., Wada, K., Watanabe, S., Matsuhashi, S., Takahashi, M., Nakanishi, H., Mori, S., & Nishizawa, N. K. (2006). Rice plants take up iron as an Fe^{3+}-phytosiderophore and as Fe^{2+}. *The Plant Journal* **45,** 335-346.

Ivanov, R., Brumbarova, T., & Bauer, P. (2012). Fitting into the harsh reality: regulation of iron-deficiency responses in dicotyledonous plants. *Molecular Plant* **5,** 27-42.

Jeong, J., & Guerinot, M. L. (2009). Homing in on iron homeostasis in plants. *Trends in Plant Science* **14,** 280-285.

Jeong, J., Merkovich, A., Clyne, M., & Connolly, E. L. (2017). Directing iron transport in dicots: regulation of iron acquisition and translocation. *Current Opinion in Plant Biology* **39,**106-113.

Kobayashi, T., & Nishizawa, N. K. (2012). Iron uptake, translocation, and regulation in higher plants.*Annual review of plant biology* **63,** 131-152.

Krauss, A. (1978). Tuberization and abscisic acid content in Solanum tuberosum as affected by nitrogen nutrition. *Potato Research* **21,**183-193.

Kumar, R. K., Chu, H. H., Abundis, C., Vasques, K., Rodriguez, D. C., Chia, J. C., Huang, R., Vatamaniuk, O. K., & Walker, E. L. (2017). Iron-nicotianamine transporters are required for proper long-distance iron

signaling. *Plant physiology* **175** , 1254-1268.

Lei, G. J., Zhu, X. F., Wang, Z. W., Dong, F., Dong, N. Y., & Zheng, S. J. (2014). Abscisic acid alleviates iron deficiency by promoting root iron reutilization and transport from root to shoot in A rabidopsis.*Plant, cell & environment* **37,** 852-863.

Lingam, S., Mohrbacher, J., Brumbarova, T., Potuschak, T., Fink-Straube, C., Blondet, E., Genschik, P., & Bauer, P. (2011). Interaction between the bHLH transcription factor FIT and ethylene insensitive3/ethylene intensive3-like1 reveals molecular linkage between the regulation of iron acquisition and ethylene signaling in Arabidopsis. *The Plant Cell* **23,** 1815-1829.

Liu, K. H., Niu, Y., Konishi, M., Wu, Y., Du, H., Chung, H. S., Lei Li, l., Boudsocq, M., McCormack, M., Maekawa, S., Ishida, T., Zhang, C., Shokat, K., Yanagisawa, S., & Sheen, J. (2017). Discovery of nitrate–CPK–NLP signalling in central nutrient–growth networks.*Nature* **545,** 311.

Li, X., Zhang, H., Ai, Q., Liang, G., & Yu, D. (2016). Two bHLH transcription factors, bHLH34 and bHLH104, regulate iron homeostasis in Arabidopsis thaliana. *Plant Physiology* **170,** 2478-2493.

Lucena, C., Waters, B. M., Romera, F. J., Garcia, M. J., Morales, M., Alcantara, E., & Perez-Vicente, R. (2006). Ethylene could influence ferric reductase, iron transporter, and H_+^-ATPase gene expression by affecting FER (or FER-like) gene activity. *Journal of Experimental Botany***57,** 4145-4154.

Ma, F., Jazmin, L. J., Young, J. D., & Allen, D. K. (2014). Isotopically nonstationary ^{13}C flux analysis of changes in Arabidopsis thaliana leaf metabolism due to high light acclimation. *Proceedings of the National Academy of Sciences***111,** 16967-16972.

Ma, F., Jazmin, L. J., Young, J. D., & Allen, D. K. (2017). Isotopically nonstationary metabolic flux analysis (INST-MFA) of photosynthesis and photorespiration in plants. In Photorespiration (pp. 167-194). Humana Press, New York, NY.

Magomya, A. M., Kubmarawa, D., Ndahi, J. A., & Yebpella, G. G. (2014). Determination of plant proteins via the kjeldahl method and amino acid analysis: a comparative study. I*nternational journal of scientific & technology research* **3,** 68-72.

Marschner, H. (2011). Marschner's mineral nutrition of higher plants. Academic press, San Diego, CA.

Miyawaki, K., Matsumoto-Kitano, M., & Kakimoto, T. (2004). Expression of cytokinin biosynthetic isopentenyltransferase genes in Arabidopsis: tissue specificity and regulation by auxin, cytokinin, and nitrate.*The plant journal* **37** , 128-138.

Mora-Macias, J., Ojeda-Rivera, J. O., Gutierrez-Alanis, D., Yong-Villalobos, L., Oropeza-Aburto, A., Raya-Gonzalez, J., Jimenez-Dominguez, G., Chavez-Calvilloa, G., Rellan-Alvareza, R., & Herrera-Estrellaa, L. (2017). Malate-dependent Fe accumulation is a critical checkpoint in the root developmental response to low phosphate. Proceedings of the National Academy of Sciences-USA, 114(17), E3563-E3572.

Morrissey, J., Baxter, I. R., Lee, J., Li, L., Lahner, B., Grotz, N., Kaplan, J., Salt, D. E., & Guerinota, M. L. (2009). The ferroportin metal efflux proteins function in iron and cobalt homeostasis in Arabidopsis. *The Plant Cell* **21,** 3326-3338.

Mukherjee, I., Campbell, N. H., Ash, J. S., & Connolly, E. L. (2006). Expression profiling of the Arabidopsis ferric chelate reductase (FRO) gene family reveals differential regulation by iron and copper.*Planta* **223** , 1178-1190.

Murashige T. & Skoog F. (1962) A revised medium for rapid growth and bioassays with tobacco tissue culture. *Biologia Plantarum***15,** 473–496.

Palmer, C. M., Hindt, M. N., Schmidt, H., Clemens, S., & Guerinot, M. L. (2013). MYB10 and MYB72 are required for growth under iron-limiting conditions. *PLoS Genetics***9,** e1003953.

Porra, R. J., Thompson, W. A., & Kriedemann, P. E. (1989). Determination of accurate extinction coefficients and simultaneous equations for assaying chlorophylls a and b extracted with four different solvents: verification of the concentration of chlorophyll standards by atomic absorption spectroscopy. *Biochimica et Biophysica Acta (BBA)-Bioenergetics* **975,** 384-394.

Rajniak, J., Giehl, R. F., Chang, E., Murgia, I., von Wiren, N., & Sattely, E. S. (2018). Biosynthesis of redox-active metabolites in response to iron deficiency in plants. *Nature chemical biology* **14** , 442-450.

Rellan-Alvarez, J., Giner-Martinez-Sierra, J., Orduna,J., Orera, I., Rodriguez-Castrillon, J.A., Garcia-Alonso, J.I., Abadia, J. & Alvarez-Fernandez, A. (2010) Identification of a tri-iron (III), tri-citrate complex in the xylem sap of iron-deficient tomato resupplied with iron: new insights into plant iron long-distance transport.*Plant and Cell Physiology* **51** , 91-102.

Robinson, N. J., Procter, C. M., Connolly, E. L., & Guerinot, M. L. (1999). A ferric-chelate reductase for iron uptake from soils.*Nature* **397** , 694-697.

Romera, F. J., Lucena, C., Garcia, M. J., Alcantara, E., & Perez-Vicente, R. (2017). The role of ethylene and other signals in the regulation of Fe deficiency responses by dicot plants. In Stress Signaling in Plants: Genomics and Proteomics Perspective, Volume 2 (pp. 277-300). Springer, Cham.

Romheld, V., & Marschner, H. (1986). Evidence for a specific uptake system for iron phytosiderophores in roots of grasses. *Plant Physiology* **80,** 175-180.

Roschzttardtz, H., Seguela-Arnaud, M., Briat, J. F., Vert, G., & Curie, C. (2011). The FRD3 citrate effluxer promotes iron nutrition between symplastically disconnected tissues throughout Arabidopsis development.*The Plant Cell* **23** , 2725-2737.

Santi, S., & Schmidt, W. (2008). Laser microdissection-assisted analysis of the functional fate of iron deficiency-induced root hairs in cucumber. *Journal of experimental botany* **59** , 697-704.

Santi, S., & Schmidt, W. (2009). Dissecting iron deficiency-induced proton extrusion in Arabidopsis roots. *New Phytologist***183,** 1072-1084.

Schikora, A., & Schmidt, W. (2001). Iron stress-induced changes in root epidermal cell fate are regulated independently from physiological responses to low iron availability. *Plant Physiology***125,** 1679-1687.

Scheible, W. R., Gonzalez-Fontes, A., Lauerer, M., Muller-Rober, B., Caboche, M., & Stitt, M. (1997). Nitrate acts as a signal to induce organic acid metabolism and repress starch metabolism in tobacco. *The Plant Cell* **9** , 783-798.

Scheible, W. R., Morcuende, R., Czechowski, T., Fritz, C., Osuna, D., Palacios-Rojas, N., Schindelasch, D., Thimm, O., Udvardi, M. K., & Stitt, M. (2004). Genome-wide reprogramming of primary and secondary metabolism, protein synthesis, cellular growth processes, and the regulatory infrastructure of Arabidopsis in response to nitrogen.*Plant physiology* **136** , 2483-2499.

Schmid, N. B., Giehl, R. F., Doll, S., Mock, H. P., Strehmel, N., Scheel, D., Kong, X., Hider, R. C., & von Wiren, N. (2014). Feruloyl-CoA 6'-Hydroxylase1-dependent coumarins mediate iron acquisition from alkaline substrates in Arabidopsis. *Plant Physiology* **164** , 160-172.

Seguela, M., Briat, J. F., Vert, G., & Curie, C. (2008). Cytokinins negatively regulate the root iron uptake machinery in Arabidopsis through a growth-dependent pathway. *The Plant Journal***55** , 289-300.

Siwinska, J., Siatkowska, K., Olry, A., Grosjean, J., Hehn, A., Bourgaud, F., Meharg, A. A, Carey, M., Lojkowska, E., & Ihnatowicz, A. (2018). Scopoletin 8-hydroxylase: a novel enzyme involved in coumarin biosynthesis and iron-deficiency responses in Arabidopsis. *Journal of experimental botany* **69** , 1735-1748.

Smolders, A. J. P., Hendriks, R. J. J., Campschreur, H. M., & Roelofs, J. G. M. (1997). Nitrate induced iron deficiency chlorosis in Juncus acutiflorus. Plant and Soil 196, 37-45.

Stacey, M. G., Patel, A., McClain, W. E., Mathieu, M., Remley, M., Rogers, E. E., Gassmann, W., Blevins, D. G., & Stacey, G. (2008). The Arabidopsis AtOPT3 protein functions in metal homeostasis and movement of iron to developing seeds. *Plant physiology* **146,**589-601.

Takei, K., Ueda, N., Aoki, K., Kuromori, T., Hirayama, T., Shinozaki, K., Yamaya, T., & Sakakibara, H. (2004). AtIPT3 is a key determinant of nitrate-dependent cytokinin biosynthesis in Arabidopsis. *Plant and Cell Physiology***45** , 1053-1062.

Teplova, I., Veselov, S., & Kudoyarova, G. (1998). Changes in ABA and IAA content in the roots and shoots of wheat seedlings under nitrogen deficiency. In Root Demographics and Their Efficiencies in Sustainable Agriculture, Grasslands and Forest Ecosystems (pp. 599-605). Springer, Dordrecht.

Tissot, N., Robe, K., Gao, F., Grant-Grant, S., Boucherez, J., Bellegarde, F., Maghiaoui, A., Marcelin, R., Izquierdo, E., Benhamed, M., Martin, A., Vignols, F., Roschzttardtz, H., Gaymard, F., Briat, J. F., & Dubos, C. (2019). Transcriptional integration of the responses to iron availability in Arabidopsis by the bHLH factor ILR3. *New Phytologist* **223** , 1433-1446.

Tsai, H. H., Rodriguez-Celma, J., Lan, P., Wu, Y. C., Velez-Bermudez, I. C., & Schmidt, W. (2018). Scopoletin 8-hydroxylase-mediated fraxetin production is crucial for iron mobilization. *Plant Physiology***177** , 194-207.

Wang, F. P., Wang, X. F., Zhang, J., Ma, F., & Hao, Y. J. (2018). MdMYB58 modulates Fe homeostasis by directly binding to the MdMATE43 promoter in plants. *Plant and Cell Physiology* **59** , 2476-2489.

Wang, Y. H., Garvin, D. F., & Kochian, L. V. (2001). Nitrate-induced genes in tomato roots. Array analysis reveals novel genes that may play a role in nitrogen nutrition. *Plant Physiology* **127** , 345-359.

Waters, B. M., Chu, H. H., DiDonato, R. J., Roberts, L. A., Eisley, R. B., Lahner, B., Salt, D. E., & Walker, E. L. (2006). Mutations in Arabidopsis yellow stripe-like1 and yellow stripe-like3 reveal their roles in metal ion homeostasis and loading of metal ions in seeds. *Plant Physiology* **141,** 1446-1458.

Wintz, H., Fox, T., Wu, Y. Y., Feng, V., Chen, W., Chang, H. S., Zhu, T., & Vulpe, C. (2003). Expression profiles of Arabidopsis thaliana in mineral deficiencies reveal novel transporters involved in metal homeostasis. *Journal of Biological Chemistry* **278** , 47644-47653.

Wu, J., Wang, C., Zheng, L., Wang, L., Chen, Y., Whelan, J., & Shou, H. (2011). Ethylene is involved in the regulation of iron homeostasis by regulating the expression of iron-acquisition-related genes in Oryza sativa. *Journal of experimental botany* **62,** 667-674.

Wu, T. Y., Gruissem, W., & Bhullar, N. K. (2018). Facilitated citrate-dependent iron translocation increases rice endosperm iron and zinc concentrations. *Plant science* **270** , 13-22.

Yan, D., Easwaran, V., Chau, V., Okamoto, M., Ierullo, M., Kimura, M., Endo, A., Yano, R., Pasha, A., Gong, Y., Bi, Y. M., Provart, N., Guttman, D., Krapp, A., Rothstein, S. J., & Nambara, E. (2016). NIN-like protein 8 is a master regulator of nitrate-promoted seed germination in Arabidopsis. *Nature Communications* **7,**13179.

Yan, J. Y., Li, C. X., Sun, L., Ren, J. Y., Li, G. X., Ding, Z. J., & Zheng, S. J. (2016). A WRKY transcription factor regulates Fe translocation under Fe deficiency. *Plant physiology* **171** , 2017-2027.

Zamioudis, C., Hanson, J., & Pieterse, C. M. (2014). β-Glucosidase BGLU 42 is a MYB 72-dependent key regulator of rhizobacteria-induced systemic resistance and modulates iron deficiency responses in A rabidopsis roots. *New Phytologist* , **204** , 368-379.

Zhao, Q., Ren, Y. R., Wang, Q. J., Yao, Y. X., You, C. X., & Hao, Y. J. (2016a). Overexpression of Mdb HLH 104 gene enhances the tolerance to iron deficiency in apple. *Plant biotechnology journal***14** , 1633-1645.

Zhao, Q., Ren, Y. R., Wang, Q. J., Wang, X. F., You, C. X., & Hao, Y. J. (2016b). Ubiquitination-related MdBT scaffold proteins target a bHLH transcription factor for iron homeostasis. *Plant physiology***172** ,

1973-1988.

Zhang, J., Liu, B., Li, M., Feng, D., Jin, H., Wang, P., Liu, J., Xiong, F., Wang, J., & Wang, H. B. (2015). The bHLH transcription factor bHLH104 interacts with IAA-LEUCINE RESISTANT3 and modulates iron homeostasis in Arabidopsis. *The Plant Cell* **27,** 787-805.

Zheng, L., Huang, F., Narsai, R., Wu, J., Giraud, E., He, F., Cheng, L., Wang, F., Wu, P., Whelan, J., & Shou, H. (2009). Physiological and transcriptome analysis of iron and phosphorus interaction in rice seedlings. *Plant Physiology* **151** , 262-274.

ZhongYang quanwei. The effect of long-term nitrogen fertilization on soil carbon balance and stability mechanism in wheat field. [D]. North West Agriculture and Forestry University. 2016 (in Chinese).

Zhou, L. J., Zhang, C. L., Zhang, R. F., Wang, G. L., Li, Y. Y., & Hao, Y. J. (2019). The SUMO E3 ligase MdSIZ1 targets MdbHLH104 to regulate plasma membrane H^+-ATPase activity and iron homeostasis. *Plant physiology* **179** , 88-106.

Zhu, X. F., Wu, Q., Zheng, L., & Shen, R. F. (2017). NaCl alleviates iron deficiency through facilitating root cell wall iron reutilization and its translocation to the shoot in Arabidopsis thaliana. *Plant and Soil* **417,** 155-167.

Acknowledgment

Author Contributions

Y.-J. H., X.-F. W., W.-J. S. conceived the study and wrote the manuscript. W.-J. S., X.-L. J., J.-C. Z., Z.-Q. F. performed mass spec, W.-J. S, J.-C. Z., Z.-Q. F. performed metal content and nitrogen content analysis experiments, W.-J. S., Z.-Q. F., C.-X. Y., W.-J. H. performed phenotypic analysis and field experiments, W.-J. S., X. W., Z.-Q. F. performed the qPCR and the RNA-Seq experiments, W.-J. S., X.-L. J., Z.-Q. F., C.-X. Y. performed the chlorophyll, pH and FCR analysis experiments.

Competing interests

The named authors declare no conflict of interest, financial or otherwise related to this work.

Figure Legend

Figure 1 . Effects of different nitrate treatment on chlorophyll and soluble Fe content. The phenotypes (a, b), the chlorophyll content of young leaves (c), and the soluble Fe content of young leaves (d) and roots (e) of 6-week-old seedlings grown in vermiculite treated with 15 mM KNO_3+ 50 µM Fe, 0.5 mM KNO_3 + 50 µM Fe, 15 mM KNO_3 +200 µM ferrozine (FRZ), 0.5 mM KNO_3 + 200 µM ferrozine (FRZ) for two weeks were showed. Error bars represent standard deviation (n[?]3). Different letters represent significantly different values at *P<0.05* .

Figure 2 . Effects of different nitrate treatment on Fe deficiency responses. FCR activity (a, b) and the pH of the treatment solution (c, d, e) of 6-week-old seedlings treated with 15 mM KNO_3 + 50 µM Fe, 0.5 mM KNO_3 + 50 µM Fe, 15 mM KNO_3 +200 µM ferrozine, 0.5 mM KNO_3 + 200 µM ferrozine for the indicated time are shown. Error bars represent standard deviation (n[?]3). * represents significantly different values at *P<0.05* .

Figure 3 . Effects of different nitrate treatment on Fe translocation from root to shoot. Total Fe content of leaves (a) and roots (b), and the Fe concentration in stems (c) of 6-week-old seedlings treated with 15 mM KNO_3 + 50 µM Fe, 0.5 mM KNO_3 + 50 µM Fe, 15 mM KNO_3 +200 µM ferrozine, 0.5 mM KNO_3 +

16

200 μM ferrozine for two weeks. Error bars represent standard deviation (n[?]6). Seedlings of same growth status were treated with 0.5 mM KNO_3 + 50 μM Fe, 15 mM KNO_3 + 50 μM Fe, 0.5 mM KNO_3 -Fe (-Fe solution supplemented with 200 μM ferrozine) or 15 mM KNO_3 -Fe (-Fe solution supplemented with 200 μM ferrozine) solutions for 1, 3, 5 and 7 days, respectively. Relative expression level of *MdFRD3* (d), *MdMATE43* (e),*MdNAS1* (f) were detected. Different letters represent significantly different values at *P<0.05* .

Figure 4 .Nitrate alleviate iron deficiency partially through citrate. Citrate content (a) and malate content (b) in roots. 6-week-old seedlings were treated with 15 mM KNO_3 + 50 μM Fe, 0.5 mM KNO_3 + 50 μM Fe, 15 mM KNO_3 + 200 μM ferrozine, 0.5 mM KNO_3 + 200 μM ferrozine for two weeks. Error bars represent standard deviation (n[?]3). Phenotype of exogenous 0.5 mM citrate treatment seedlings(c), chlorophyll content of young leaves (d), total Fe content of leaves (e) and roots (f) of 6-week-old seedlings treated with 15 mM KNO_3 + 200 μM ferrozine, 15 mM KNO_3 + 200 μM ferrozine + 0.5 mM citrate (CIT), 0.5 mM KNO_3 + 200 μM ferrozine, 0.5 mM KNO_3+ 200 μM ferrozine + 0.5 mM citrate (CIT) for 3 weeks. Error bars represent standard deviation (n[?]3). Different letters represent significantly different values at *P<0.05* .

Figure 5 . Differentially expressed genes analysis of different nitrate treatment using RNA-seq. Differently expressed gene number of roots (a) of 6-week-old seedlings treated with 15 mM KNO_3 and 15 mM KCl for 24 hours. Fe-related differently expressed genes of roots (b). S1, S2, S3 represent 3 biological repeats. The data were filtered at |Foldchange|[?]1.5,*pval<0.05* .

Figure 6 . Relative expression level of Fe-related genes in response to LN and HN in roots. Seedlings of same growth status were treated with 0.5 mM KNO_3 + 50 μM Fe, 15 mM KNO_3 + 50 μM Fe, 0.5 mM KNO_3 -Fe (-Fe solution supplemented with 200 μM ferrozine) or 15 mM KNO_3 -Fe (-Fe solution supplemented with 200 μM ferrozine) solutions for 1, 3, 5 and 7 days, respectively. Relative expression level of *MdFIT* (a), *MdFER1* (b), *MdYSL3*(c), *MdYSL1* (d), *MdCYP82C4* (e), *MdNRAMP1* (f),*MdAHA2* (g) and *MdFRO2* (h) were detected. MdActin was selected as a control gene. Results were based on the average of three replicate experiments. Different letters represent significantly different values at *P<0.05* .

Figure 7 . ABA alleviates nitrate-mediated Fe deficiency response. ABA content in young leaves (a) and roots (b) of 6-week-old seedlings treated with 15 mM KNO_3 + 50 μM Fe, 0.5 mM KNO_3 + 50 μM Fe, 15 mM KNO_3 +200 μM ferrozine, 0.5 mM KNO_3 + 200 μM ferrozine for the indicated time are shown. Chlorophyll content of young leaves (c) and phenotypes of exogenous 1μM ABA treatment (d). Error bars represent standard deviation (n[?]4). Different letters represent significantly different values at *P<0.05* .

Figure 8 . The regulatory mechanism on nitrate-mediated iron deficiency response is conserved in *Arabidopsis thaliana* . Phenotype (a, b), chlorophyll content (c) and total Fe content of shoot (d) of 2-week-old seedlings treated with 20 mM KNO_3 + 50 μM Fe, 0.2 mM KNO_3 + 50 μM Fe, 20 mM KNO_3 +200 μM ferrozine, 0.2 mM KNO_3 + 200 μM ferrozine for one week. Error bars represent standard deviation (n[?]3). Different letters represent significantly different values at*P<0.05* .

Figure 9 . A model of nitrate in regulation of iron deficiency. NO_3^- is a member of substrates that affect plant iron deficiency response, both in direct and indirect ways. On the one hand, LN treatment helped to rhizosphere acidification and increase the solubility of Fe in rhizosphere. LN treatment increased the expression of genes including *MdFRD3* , *MdMATE43* ,*MdNRAMP1* , *MdNRAMP6* , *MdNAS1* , *MdYSL1* ,*MdYSL3* that are critical for Fe transport, and *MdFIT* which could activate expression of downstream genes to positively regulate Fe deficiency. On the other hand, LN treatment increased the citrate and ABA content in roots under Fe deprivation conditions, which contribute to Fe transportation and homeostasis. Dotted line represents the results of previous study (Lei et al. 2014). Yellow arrows represent metabolism pathway.

Figure S1 . Effect of applicating nitrate on the Fe deficiency symptoms in the young leaves of apple. 2-year-old 'Fuji' apple trees treated with 10g KNO3/per plant, 30g KNO3/per plant, 60g KNO3/per plant, 120g KNO3/per plant for 3 months. Phenotypes of young leaves (a, b, c, d) and whole trees (e, f, g, h). Each line contains 11 trees. Each treatment contains 11 plants.

Figure S2 . Chlorophyll content of young leaves of 2-year-old 'Fuji' apple trees treated with different concentration of nitrate. Error bars represent standard deviation (n=5). Different letters represent significantly different values at *P<0.05* .

Figure S3 . Nitrogen content of differently treated seedlings. NO_3^- content of roots (a), leaves (b) and total nitrogen content of leaves and roots (c) of 6-week-old seedlings treated with 15 mM KNO_3 + 50 μM Fe, 0.5 mM KNO_3 + 50 μM Fe, 15 mM KNO_3 + 200 μM ferrozine, 0.5 mM KNO_3 + 200 μM ferrozine for two weeks. Error bars represent standard deviation (n=3). Different letters represent significantly different values at *P<0.05* .
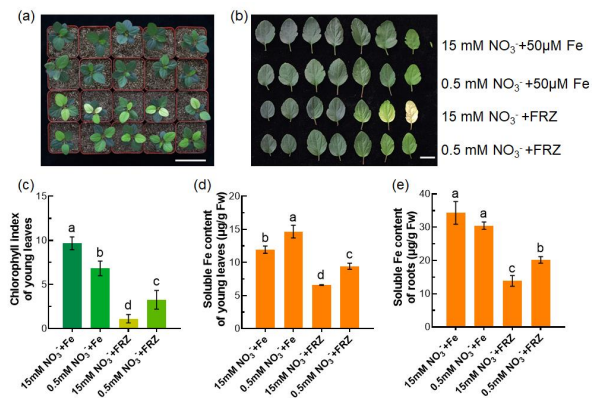
Figure S4 . Effects of different nitrate treatment on citrate content (a) and malate content (b) in leaves. 6-week-old seedlings were treated with 15 mM KNO_3 + 50 μM Fe, 0.5 mM KNO_3 + 50 μM Fe, 15 mM KNO_3 +200 μM ferrozine, 0.5 mM KNO_3 + 200 μM ferrozine for two weeks. Error bars represent standard deviation (n[?]3). Different letters represent significantly different values at *P<0.05* .

Figure S5 . Nitrate regulates metal ion and phytohormone related genes expression. Number of metal ion-related genes regulated by nitrate (a) and number of phytohormone related genes regulated by nitrate (b) in roots. The data were filtered at |Foldchange|[?]1.5,*pval<0.05* .

Fig S6 . ABA biosynthesis and signal pathway genes which are regulated by nitrate. S1, S2, S3 represent 3 biological repeats. The data were filtered at |Foldchange|[?]1.5,*pval<0.05* .

Table 1 qRT-PCR Primers used in this study

Primer name	Primer sequence_F	Primer sequence_R
MdActin	GGACAGCGAGGACATTCAGC	CTGACCCATTCCAACCATAACA
MdFRD3	TACAAGCGTGTTTTCAAATGGGATA	CTTTCGCAGATTCCACGTTCATTT
MdMATE43	AAGTGGAAGATGCCTGTTGGTGTT	CTTTTCCCGCTTCTCACCTTTCGC
MdNAS1	CCCTCCCAAGATGTCAACATGCTC	ACAAAGGCAATTTTGCTAGGCACA
MdFIT	GTCAAGCTGGTTCTACTACTCCA	TGTTAGGAACTAAAGACCGCAAT
MdFER1	CGGGACAATGGTGGTGCTGTTAG	TTATGGCGGCTTCGGACTCTTTT
MdYSL1	ATACAATAAACGGCTAGGATGTG	CAAGTAACTAAAGAAGGCAAGGA
MdYSL3	ATCATCCCGCTTATGTTTCCTCA	CAGACCACAGCCTACAAGTCCAG
MdCYP82C4	TCTGCCTTATGCAAACTCTATCA	CACTGCTGCTTATCACCAACGAC
MdNRAMP1	GACTATTTGGTAGCGAAGATGTG	AAACAAGTGATAGACACGGACAA
MdAHA2	AGCCTGGAGGAGATCAAGAACGAG	AAAATCTTGCCAATCTGGCGGCTT
MdFRO2	AATCAGACGAAAGGCTAACTCAA	GAAGATAGATACAACCCAACACC

Figure 1. Effects of different nitrate treatment on chlorophyll and soluble Fe content. The phenotypes (a, b), the chlorophyll content of young leaves (c), and the soluble Fe content of young leaves (d) and roots (e) of 6-week-old seedlings grown in vermiculite treated with 15 mM KNO_3 + 50 µM Fe, 0.5 mM KNO_3 + 50 µM Fe, 15 mM KNO_3 +200 µM ferrozine (FRZ), 0.5 mM KNO_3 + 200 µM ferrozine (FRZ) for two weeks were showed. Error bars represent standard deviation (n≥3). Different letters represent significantly different values at *P<0.05*.

Hosted file

`Figures.pdf` available at https://authorea.com/users/313412/articles/443919-low-nitrate-alleviates-iron-deficiency-through-regulating-iron-homeostasis-in-apple